

## Ultrasensitive near-infrared cavity ring-down spectrometer for precise line profile measurement

Bo Gao, Wei Jiang, An-Wen Liu, Yan Lu, Cun-Feng Cheng,  
Guo-Sheng Cheng, and Shui-Ming Hu<sup>a)</sup>

*Department of Chemical Physics, Hefei National Laboratory for Physical Sciences at the Microscale,  
University of Science and Technology of China, Hefei 230026, China*

(Received 2 November 2009; accepted 17 March 2010; published online 15 April 2010)

A cavity ring-down (CRD) spectrometer is built with a continuous-wave Ti:sapphire ring laser. Using a pair of  $R \sim 0.999\,95$  high-reflective mirrors, the noise-equivalent minimum detectable absorption loss reaches  $7 \times 10^{-11}/\text{cm}$  over the spectral range of 780–830 nm. A thermal-stabilized Fabry-Perot interferometer is applied to calibrate the CRD spectrum with an accuracy of  $1 \times 10^{-4} \text{ cm}^{-1}$ . The quantitative measurement is carried out for the line profile measurements of some overtone absorption lines of  $\text{C}_2\text{H}_2$  near 787 nm. Doppler determined line shape has been observed with milli-Torr acetylene gas in the ring-down cavity. The instrumental line width is estimated from the line profile fitting to be  $<1 \times 10^{-4} \text{ cm}^{-1}$ . It demonstrates that the CRD spectrometer with extremely high sensitivity is also very suitable for quantitative measurements including precise line profile studies in the near-infrared. © 2010 American Institute of Physics. [doi:10.1063/1.3385675]

### I. INTRODUCTION

The molecular spectral line profile data is essential in the studies of the atmospheric absorption modeling<sup>1</sup> and the investigations of intermolecular interactions.<sup>2,3</sup> Daussy *et al.*<sup>4</sup> proposed to determine the Boltzmann constant from the precise measurement of the Doppler line width of a molecular line in the midinfrared (mid-ir) region. For the purpose of line profile studies, a frequency precision at the level of  $10^{-3} \text{ cm}^{-1}$  or higher is necessary which is beyond the possible spectral resolution of the available dispersion spectrometers or Fourier transform interferometers. In this case, spectroscopy based on tunable lasers will be the best choice. The excellent performance of the near infrared lasers gives the possibility to measure the line profile with sufficient precision. However, compared with those spectrometers working with mid-ir lasers,<sup>5,6</sup> because the molecular line intensity drops several to (typically more than three) orders of magnitudes in the near-ir region, a more sensitive method should be applied.

Since 1988,<sup>7</sup> cavity ring-down spectroscopy (CRDS) has been introduced as a powerful tool for gas-phase applications requiring high sensitivity detection, such as recording weak bands of small molecules,<sup>8,9</sup> detection of trace gas,<sup>10,11</sup> and experiments in molecular beams.<sup>12–14</sup> The fundamentals of the technique and its different experimental implementations have been reviewed in many publications<sup>15–20</sup> and books.<sup>21,22</sup> The main idea of this method is to measure the decay rate of the light (often laser) inside a resonant cavity composed of two high-reflectivity mirrors. The decay rate  $1/\tau$ , where  $\tau$  is the “ring-down time,” is proportional to the total optical losses inside the cavity. The ring-down time of an empty cavity is related to the reflectivity of the cavity mirrors

$$\tau = \frac{L}{c} \left( \frac{\sqrt{R_1 R_2}}{1 - \sqrt{R_1 R_2}} \right), \quad (1)$$

where  $L$  is the length of the cavity,  $c$  is the speed of light, and  $R_1$  and  $R_2$  are reflectivity of two cavity mirrors. In the case of  $R_1 = R_2 = R \approx 1$ ,  $\tau \approx L/c(1-R)$ . The sample absorption coefficient can be retrieved from the difference of the decay rates between an empty cavity and a cavity containing the sample

$$\alpha = \frac{1}{c} \left( \frac{1}{\tau} - \frac{1}{\tau_0} \right), \quad (2)$$

where  $\tau$  and  $\tau_0$  are the decay time of the cavity with and without sample, respectively. In this case, the minimum detectable absorption loss (MDAL) can be derived from the minimum detectable change in the decay time  $\delta\tau_0$

$$\alpha_{\min} = \frac{1}{c\tau_0^2} \delta\tau_0. \quad (3)$$

The pioneer implementations of CRDS used pulsed lasers to inject light into the cavity. O’Keefe and Deacon<sup>7</sup> used a pulsed dye laser and achieved a MDAL of  $2 \times 10^{-8}/\text{cm}$ . The sensitivity of pulsed-CRDS is limited by multiple longitudinal modes excitation in the cavity which causes frequency beats to the exponential decay. In addition, the absorption coefficient of the sample will have a slightly different value at the frequency of each of the excited cavity modes. These effects limit the shot-to-shot variation in ring-down time to about 1% level. It is also an obstacle for quantitative applications to retrieve accurate absorption coefficient from the decay curve.<sup>23</sup> The spectral resolution is also often limited by the pulsed lasers (typically  $10^{-2} - 10^{-1} \text{ cm}^{-1}$ ).

Since continuous-wave (cw) lasers have very narrow line widths (megahertz or less), it allows to couple a cw single-mode laser to a single longitudinal mode of the ring-down cavity, thereby reducing the variations among different

<sup>a)</sup>Electronic mail: smhu@ustc.edu.cn.

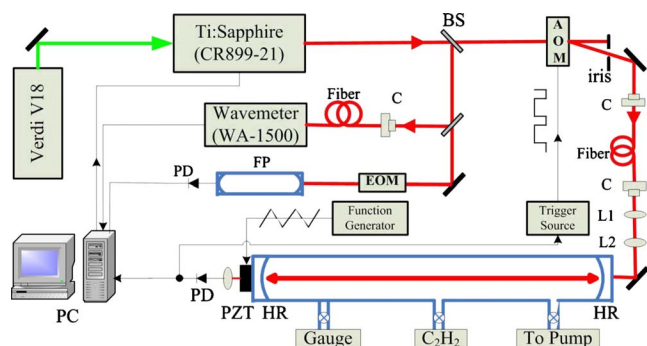


FIG. 1. (Color online) Schematic diagram of the experimental setup. The abbreviations are as following: beam splitter (BS); acousto-optical modulator (AOM); high-reflectivity mirror (HR); pinhole (PH); photodiode (PD); lens (L1,L2); fiber coupler (c); Fabry-Perot (FP) interferometer; and electro-optic modulator (EOM).

ring-down events. The first demonstration of cw-CRDS is performed by Romanini *et al.*<sup>24–26</sup> The scheme employed by Romanini<sup>24</sup> which in later years became common in cw-CRDS experiments. The cavity length is periodically modulated with a ring piezoactuator to sweep the cavity fringe over the laser line. When the intensity of light exiting the cavity reaches a predetermined threshold, the light beam will be rapidly switched off [usually using an acoustic-optical modulator (AOM)] and then the ring-down signal will be recorded and used to retrieve the decay time from exponential curve fitting. A noise-equivalent MDAL of  $2 \times 10^{-10}/\text{cm}$ , which is the best CRDS sensitivity reported to date, has been obtained by using a cw diode laser and mirrors of reflectivity  $R \sim 99.999\%$ .<sup>25</sup>

The very high sensitivity of CRDS allows to detect high overtones of molecules in the near-ir region easily. Owing to the direct-absorption character, CRDS should be also applicable for delicate quantitative measurement like precise line profile measurement. In this work, we will present our CRDS setup based on a wide tunable Ti:sapphire laser and a ring-down cavity with a pair of  $R=0.999\ 95$  mirrors. Sensitivity of  $7 \times 10^{-11}/\text{cm}$  has been achieved and the Doppler broadened line profile of very low pressure  $\text{C}_2\text{H}_2$  has been measured with  $10^{-4}\ \text{cm}^{-1}$  precision. It demonstrates the present CRDS can be applied for those quantitative measurements where both very high sensitivity and high accuracy are essential.

## II. EXPERIMENTAL SETUP

The experimental setup is presented in Fig. 1. The near-ir laser beam is from a cw tunable Ti:sapphire laser (Coherent 899-21) pumped with a 532 nm solid state laser (Coherent Verdi-18). The first order beam after an AOM (ISOMET 1205C) is introduced into a single-mode fiber. A set of lenses are used to couple the laser beam into the ring-down cavity. The cavity is 1.25 m long and the curvature radius of the high-reflectivity (HR) mirrors is 100 cm. Two HR mirrors of the high-reflectivity (HR) mirrors is 100 cm. Two HR mirrors were bought from Los Gatos Inc. and the stated reflectivity is 99.995%. Both HR mirrors are in vacuum and one is mounted on a piezoelectric actuator (Physik Instrumente GmbH). The actuator is driven with a triangle wave from a function generator.

The Ti:sapphire laser is running in a step-scan mode controlled with a personal computer (PC). On each step, the laser frequency keeps unchanged for about 0.2 s. Meanwhile, the cavity length is modulated using a 300 Hz triangle wave. Once the cavity longitudinal mode gets resonant with the laser frequency, in other words, a ring-down event occurs, the photocurrent signal obtained from the photodiode detector (PD) will increase dramatically and trig a rectangular pulse to shut off the input laser through the AOM. The photocurrent signal then decays exponentially and the ring-down signal is recorded with a 14 bit digitizer (ADLink PCI-9820) installed in the PC. Figure 2(a) shows a typical ring-down signal. The decay curve is fitted online with a least square fitting procedure. Figure 2(b) shows the residual between the experimental signal and the fitting curve ( $\Delta = \text{Exp.} - \text{Calc.}$ ). For each ring-down event, the ring-down time ( $\tau$ ) and the standard deviation of the fitting residual ( $\sigma$ ) will be given from the fitting. Within 0.2 s, typically 80 ring-down events are recorded and Fig. 2(c) shows an example of these  $\tau$  and  $\sigma$  data. It is worth noting that to reach higher sensitivity, it is desirable to carefully align the laser beam and to couple only the TEM<sub>00</sub> mode of the laser beam into the ring-down cavity. However, the alignment is very sensitive to the environmental perturbations like vibrations. Such perturbations will lead to some ring-down events with unexpected large deviations. If those data with abnormal deviations are included in the averaging process, the retrieved ring-down time will be distorted. A simple procedure is applied to automatically exclude these “perturbed events” from the averaging process. The criterion to “remove” is that whether the decay time and the fitting residual values are within three times of the standard deviation. The border of the criteria is shown with dashed lines on Fig. 2(c). In this way, the noise level of the final spectrum which is determined with the fluctuation of the averaged decay time values is estimated to be at least two times lower.

### A. Mirror reflectivity measurement and sensitivity determination

Owing to the wide tunability of the Ti:sapphire laser, the present CRDS setup can be tunable in the wide range 700–1000 nm with different mirror sets. The present CRDS cavity mirrors are coated with antireflective film with stated reflectivity of 99.995% at 790 nm. By detecting the ring-down time, the reflectivity of the mirrors is determined with Eq. (1). Due to possible misalignment, the mirror reflectivity determined with the ring-down time actually presents the lower limit of the real value. The results are shown in Fig. 3. The ring-down time varies from 60 to 75  $\mu\text{s}$  in the range 780–830 nm with the best reflectivity of 0.999 946 around 810 nm. Since the reflectivity we obtained here has been very close to the stated value given by the producer, it indicates that the optics has been well aligned in our experiment.

As given in Eq. (3), the sensitivity of the CRD spectrometer, as the MDAL, is proportional to the variance of the cavity decay rate. In the upper panel of Fig. 4, it is given a 15 min measurement of the ring-down time of the present CRDS setup. The corresponding Allan variance of the value ( $1/c\tau$ ) is given in the lower panel of the figure. It is readily

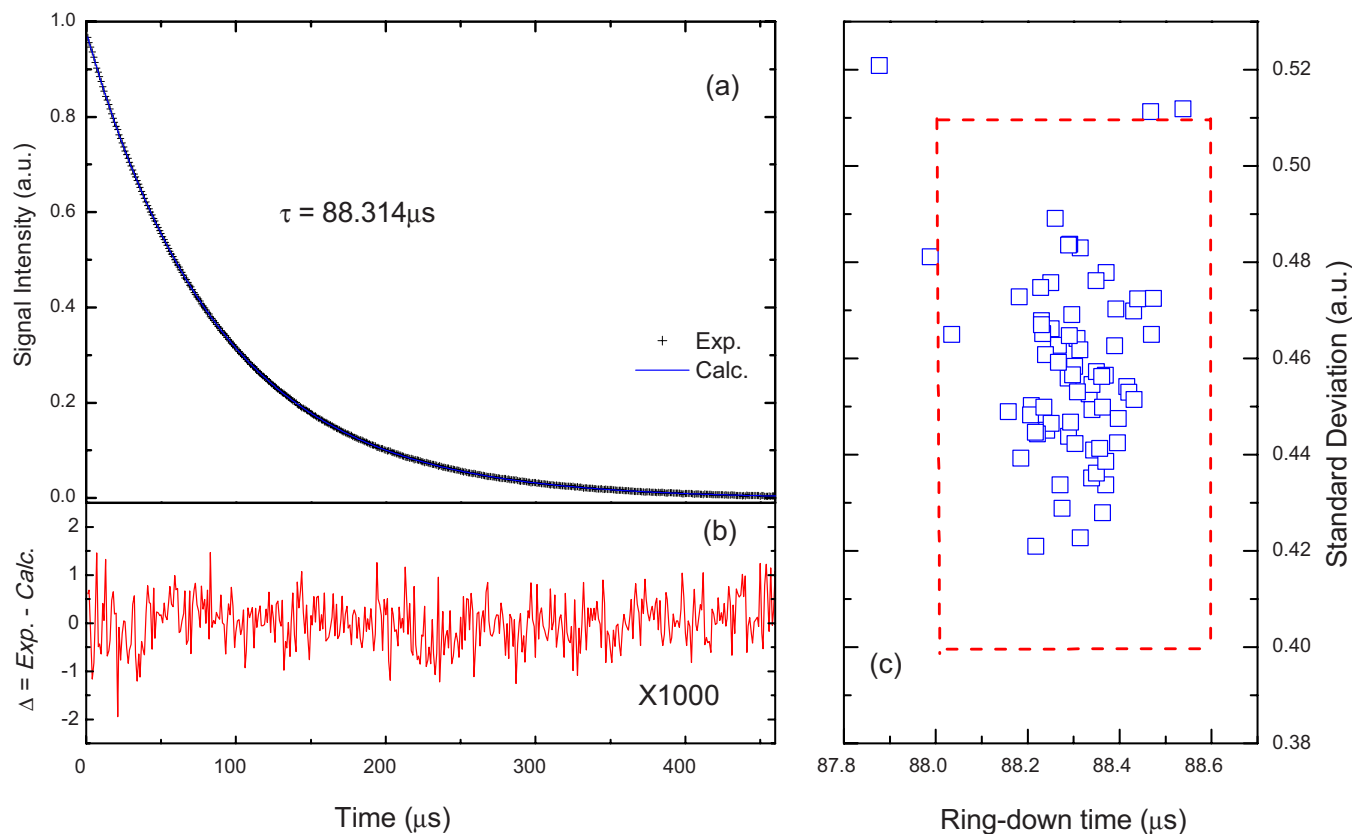


FIG. 2. (Color online) Ring-down curve (a) and the fitting residue (b) of one ring-down event. The fitting result (ring-down time) and standard deviation of the fitting are presented in (c). The criterion of the “removal” procedure (see text) is shown as dashed lines on (c).

seen that the long time drift degrades the performance. This slow drift in ring-down time ( $\sim 0.02 \mu\text{s}/\text{min}$ ) may result from the drift of the cavity length due to room temperature fluctuations. Nevertheless, since the sampling rate in the experiment is high enough that an absorption line can be measured typically within 10 s, the sensitivity of the CRDS is estimated to be  $7 \times 10^{-11}/\text{cm}$ .

### B. Spectrum calibration

A small portion of the laser beam is also sent to a  $\lambda$ -meter (Burleigh WA1500) to record the wavelength. The

stated accuracy of the  $\lambda$ -meter is  $0.002 \text{ cm}^{-1}$ , and the measurement speed of the  $\lambda$ -meter ( $\sim 1$  readout/s) is much slower than the scan speed (typically 5 steps/s). So it fails for the precise measurement where a few megahertz accuracy is necessary. An example of the  $\lambda$ -meter readouts during a scan are given in the upper panel of Fig. 5.

Here we use the sidebands produced from fast phase modulation for the calibration purpose. The sidebands are introduced through a fiber electrical-optic modulator (EOM) (Photline Inc.). Radio-frequency (RF) signal produced from

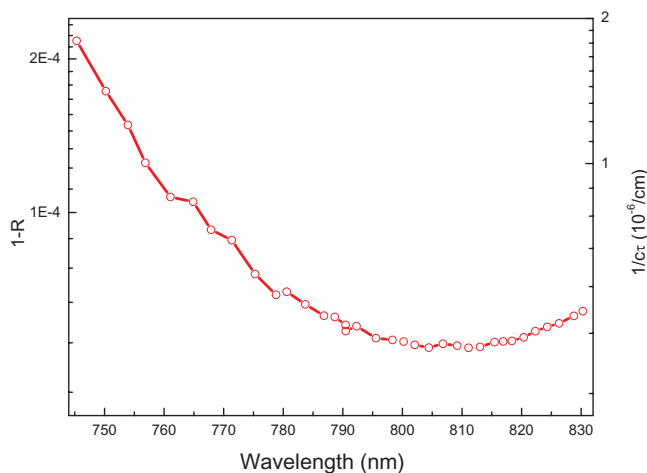


FIG. 3. (Color online) Mirror reflectivity and the ring-down time over the 745–830 nm range.

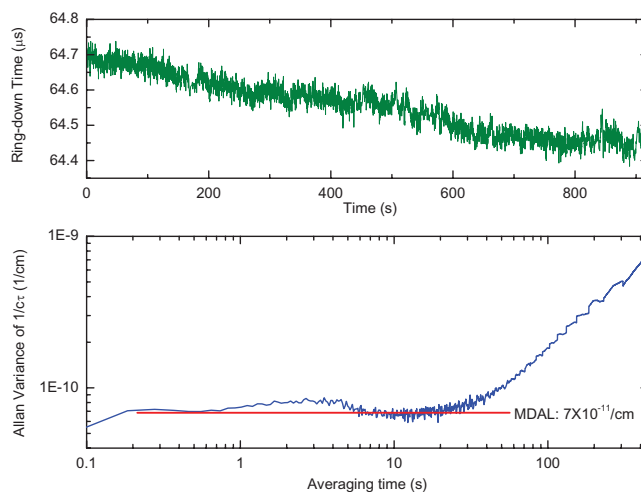


FIG. 4. (Color online) Allan variance of the decay rate ( $1/c\tau$ ) and the MDAL.

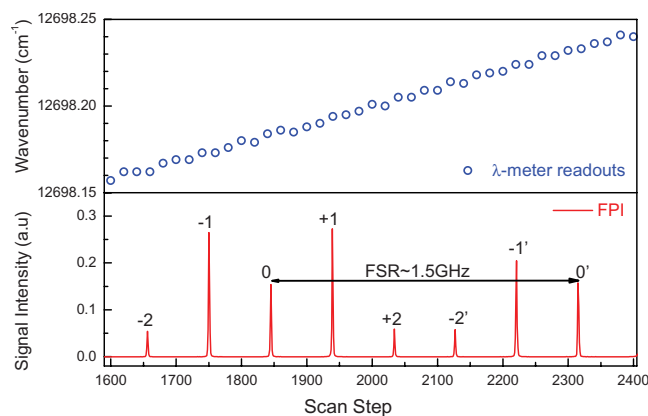


FIG. 5. (Color online) FPI fringes (lower panel) and  $\lambda$ -meter outputs (upper panel) in a scan. In the lower panel, the labels correspond to different orders of the sidebands produced with an EOM.

a frequency source (Agilent 9310A) is amplified and used to drive the EOM. The sidebands are measured with a Fabry-Perot interferometer (FPI). The free spectral range (FSR) of the FPI is 1.5 GHz and the finesse is 200. The FPI has an invar case and is nearly zero-expansion using the negative thermal coefficients of expansion of the internal piezostacks. The FPI is put in a vacuum stainless steel chamber to avoid the change of the cavity length due to temperature fluctuations or sound induced vibrations. When the laser scans, the carrier, first and second order, sidebands peaks will be measured one by one through a photodetector at the end of the FPI. For illustration, the FPI signal in a scan is presented in the lower panel of Fig. 5. Using a 312.3 MHz RF source, we get about five peaks (0,  $\pm 1$ , and  $\pm 2$  orders) within a FSR of the FPI. These peaks in the FPI spectrum are recorded simultaneously with the CRDS spectrum and they are used for calibration with an accuracy about 1 MHz.

### III. LINE PROFILE MEASUREMENTS OF $C_2H_2$ NEAR 787 NM

To demonstrate the quantitative measurement capability of the present CRD spectrometer, the absorption lines of  $C_2H_2$  near 787 nm were measured. Since the  $R(9)$  line of the  $\nu_1 + 3\nu_3$  overtone band is well isolated from other lines (particularly the water lines), we pick this line for precise line profile measurement. The relatively strong  $R(9)$  line at  $12\,696.4\text{ cm}^{-1}$  allows us to observe it with very low sample pressure. A small amount of acetylene gas was filled in the cavity and soon pumped out with a mechanical pump. The residual acetylene gas pressure was estimated around a few milli-Torr which is below the detection limit of a 1 Torr full-scale capacitance manometer (MKS 627B). This low pressure allows us to detect line profile without pressure broadening. The temperature was monitored during the experiment and gave  $300 \pm 0.5\text{ K}$ .

To evaluate the precision of the CRDS spectrometer, the  $R(9)$  line has been measured with different experimental conditions. Two of the spectra are presented in Fig. 6. As in Figs. 6(a) and 6(c), the observed spectra were recorded with different laser frequency scanning steps which were  $0.0006$  and  $0.0001\text{ cm}^{-1}$  for (a) and (c), respectively. The line width

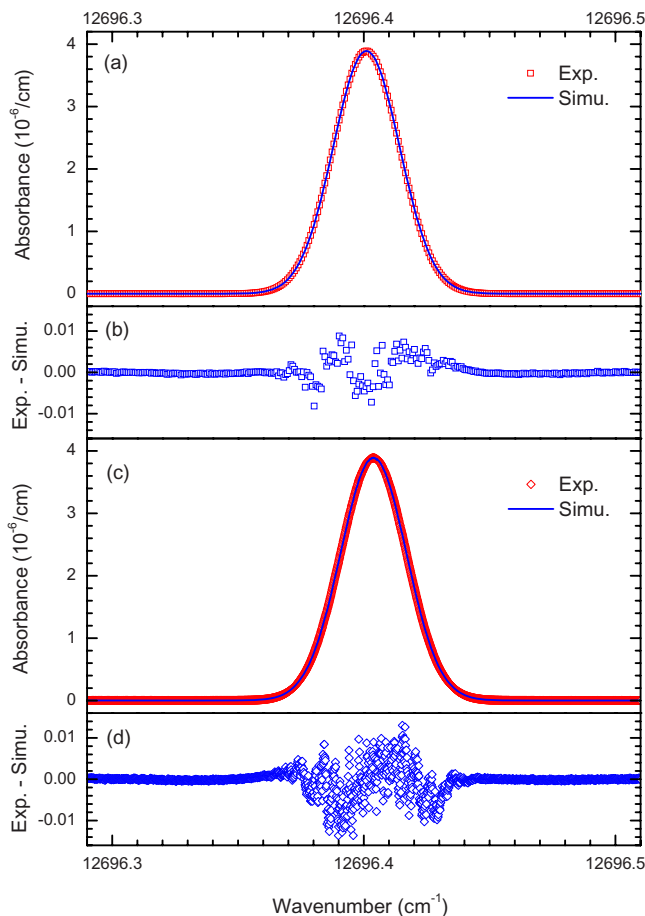


FIG. 6. (Color online) The  $C_2H_2$  absorption centered at  $12\,296.4\text{ cm}^{-1}$  recorded with different laser scanning intervals,  $0.0006$  and  $0.0001\text{ cm}^{-1}$ , respectively. The experimental data and the calculated line profiles are given in the upper panel. The residues are given in the lower panel.

is mainly determined by the Gaussian type Doppler broadening. Simulated spectra are also given in the same figure. The simulation is calculated with Voigt line profile fitting to the experimental spectrum. The fitting program is called “fityk” (<http://www.unipress.waw.pl/fityk/>) which is an interactive least square multiline fitting program based on the Levenberg–Marquardt algorithm. In the fitting, the line center, the integrated absorbance, the half width at half maximum (HWHM) of the Lorentzian and Gaussian components, and the baseline (assumed to be a straight line) can be fitted. If we fit the spectrum with the Gaussian width fixed on the theoretical Doppler width,  $0.015\,44\text{ cm}^{-1}$  HWHM at  $300\text{ K}$ , the fitted HWHM of the Lorentzian component width was  $4 \times 10^{-5}\text{ cm}^{-1}$ . The differences between the observed and simulated spectrum are presented in Figs. 6(b) and 6(d). The extremely small deviation on the baseline is consistent with the high sensitivity discussed in last section.

In fact, the line profile should be a convolution of the Doppler broadening, pressure broadening, and the instrumental line profile. Since the  $< 1\text{ Pa}$  pressure induced broadening can be neglected, the deviation of the line profile from the pure Doppler induced Gaussian profile can be an estimation of the upper limit of the instrumental line width. We also tried to fit the spectrum with a pure Gaussian function, or considering variation of the Gaussian width due to tempera-



ture fluctuation, all the fitting results showed the instrumental line width (if any) should be below  $1 \times 10^{-4} \text{ cm}^{-1}$ . Such negligible instrumental line width (several hundred times smaller than the Doppler one) is satisfied for line profile studies. It is also notable that the fitting residual at the center of the line is about 400 times smaller than the signal, but remains much larger than the noise level. It is probably a result from: (1) the fluctuation of the temperature which may cause the change of Gaussian line width of  $3 \times 10^{-5} \text{ cm}^{-1}/\text{K}$  here and (2) laser frequency drift which is estimated to be also at the  $10^{-5} \text{ cm}^{-1}$  level.

#### IV. DISCUSSION

A cavity ring-down spectrometer based on a wide tunable Ti:sapphire laser has been built and its performance has been experimentally evaluated. Using a pair of  $R \approx 0.99995$  mirrors,  $7 \times 10^{-11}/\text{cm}$  sensitivity has been obtained. Such a sensitivity corresponds to measure with a 100 km long absorption cell and with a signal-noise-ratio over 1000. Since mirrors with higher reflectivity are available nowadays, the sensitivity can be potentially pushed to higher level. Owing to the wide tunability of the Ti:sapphire ring laser, the present spectrometer can smoothly operate with  $<10^{-10}/\text{cm}$  sensitivity in a large spectral range which is only limited by the HR cavity mirrors (over 50 nm for present setup).

Moreover, the present CRDS can also be applied for quantitative measurements without sacrificing the sensitivity. Using thermostabilized etalon and EOM sidebands,  $1 \times 10^{-4} \text{ cm}^{-1}$  precision has been obtained. With the high-precision and high sensitivity advantages, the near-ir CRDS spectrometer can be applied for those precise line profile measurements interested in atmospheric or chemical kinetics studies. For example, it is very suitable to measure the extremely weak overtones of polyatomic molecules, including the weak absorption bands of water vapor. Such information is essential in setting up an accurate potential energy surface for those molecules, which is desirable to model the atmospheric absorption and the global radiation equilibrium. The spectral accuracy can be potentially improved since the cw near-ir laser is inherent with excellent frequency stability which can reach subkilohertz level by locking the laser to a frequency standard or an ultrastable Fabry-Perot cavity. In this case, CRDS using frequency locked cw-laser can be very competitive in applications which need very high spectral precision like determination of the Boltzmann constant from the Doppler line width of a molecular absorption line.

#### ACKNOWLEDGMENTS

Authors are indebted to D. Romanini and S. Kassi for helpful discussion. The work is jointly supported by NSFC (Grant Nos. 90921006, 20873132, 10728408, and 20533060), by Chinese Ministry of Science and Technology (Grant Nos. 2006CB922001 and 2007CB815203), and by the Fok Ying Dong Education Foundation (Grant No. 101013). The support of the Groupement de Recherche International SAMIA between CNRS (France) (Grant No. UMR 5588), RFBR (Russia) and CAS (China) is also acknowledged.

- <sup>1</sup>D. Mondelain, S. Payan, W. Deng, C. Camy-Peyret, D. Hurtmans, and A. W. Mantz, *J. Mol. Spectrosc.* **244**, 130 (2007).
- <sup>2</sup>R. Wehr, J. R. Drummond, and A. D. May, *Appl. Opt.* **46**, 978 (2007).
- <sup>3</sup>D. Mondelain, P. Chelin, A. Valentin, D. Hurtmans, and C. Camy-Peyret, *J. Mol. Spectrosc.* **233**, 23 (2005).
- <sup>4</sup>C. Daussy, M. Guinet, A. Amy-Klein, K. Djerroud, Y. Hermier, S. Bräu, C. J. Borde, and C. Chardonnet, *Phys. Rev. Lett.* **98**, 250801 (2007).
- <sup>5</sup>F. K. Tittel, D. Richter, and A. Fried, *Top. Appl. Phys.* **89**, 445 (2003).
- <sup>6</sup>W.-P. Deng, B. Gao, C.-F. Cheng, G.-S. Cheng, S.-M. Hu, and Q.-S. Zhu, *Rev. Sci. Instrum.* **79**, 123101 (2008).
- <sup>7</sup>A. O'Keefe and D. A. G. Deacon, *Rev. Sci. Instrum.* **59**, 2544 (1988).
- <sup>8</sup>P. Macko, D. Romanini, S. Mikhailenko, O. V. Naumenko, S. Kassi, A. Jenouvrier, V. G. Tyuterev, and A. Campargue, *J. Mol. Spectrosc.* **227**, 90 (2004).
- <sup>9</sup>S. Kassi, D. Romanini, A. Campargue, and B. Bussery-Honvault, *J. Mol. Spectrosc.* **409**, 281 (2005).
- <sup>10</sup>R. Provencal, M. Gupta, T. G. Owano, D. S. Baer, K. N. Ricci, A. O'Keefe, and J. R. Podolske, *Appl. Opt.* **44**, 6712 (2005).
- <sup>11</sup>J. M. Langridge, S. M. Ball, and R. L. Jones, *Analyst (Cambridge, U.K.)* **131**, 916 (2006).
- <sup>12</sup>T. Motylewski and H. Linnartz, *Rev. Sci. Instrum.* **70**, 1305 (1999).
- <sup>13</sup>F. Ito and T. Nakanaga, *Chem. Phys. Lett.* **318**, 571 (2000).
- <sup>14</sup>S.-H. Wu, P. Dupré, and T. A. Miller, *Phys. Chem. Chem. Phys.* **8**, 1682 (2006).
- <sup>15</sup>J. J. Scherer, J. B. Paul, A. O'Keefe, and R. J. Saykally, *Chem. Rev. (Washington, D.C.)* **97**, 25 (1997).
- <sup>16</sup>G. Berden, R. Peeters, and G. Meijer, *Int. Rev. Phys. Chem.* **172**, 565 (2000).
- <sup>17</sup>S. S. Brown, *Chem. Rev. (Washington, D.C.)* **103**, 5219 (2003).
- <sup>18</sup>S. M. Ball and R. L. Jones, *Chem. Rev. (Washington, D.C.)* **103**, 5239 (2003).
- <sup>19</sup>B. A. Paldus and A. A. Kachanov, *Can. J. Phys.* **83**, 975 (2005).
- <sup>20</sup>M. Mazurenka, A. J. Orr-Ewing, R. Peverall, and G. A. D. Ritchie, *Annu. Rep. Prog. Chem., Sect. C: Phys. Chem.* **101**, 100 (2005).
- <sup>21</sup>K. W. Busch and M. A. Busch, *Cavity-Ringdown Spectroscopy—An Ultratrace-Absorption Measurement Technique*, ACS Symposium Series (American Chemical Society, Washington, D.C., 1999), Vol. 720, pp. 7–19.
- <sup>22</sup>R. van Zee and J. Looney, *Cavity-Enhanced Spectroscopies* (Academic, New York, 2002), Vol. 40.
- <sup>23</sup>P. Zalicki and R. N. Zare, *J. Chem. Phys.* **102**, 2708 (1995).
- <sup>24</sup>D. Romanini, A. Kachanov, N. Sadeghi, and F. Stoeckel, *Chem. Phys. Lett.* **264**, 316 (1997).
- <sup>25</sup>D. Romanini, A. Kachanov, and F. Stoeckel, *Chem. Phys. Lett.* **270**, 538 (1997).
- <sup>26</sup>D. Romanini, A. Kachanov, and F. Stoeckel, *Chem. Phys. Lett.* **270**, 546 (1997).